2.12 – 2.07 Ga Late- to post-collisional peraluminous granitoid magmatism in the Marowijne Greenstone Belt of Suriname

S. C. Kromopawiro[1], S. Kroonenberg[2], L. Kriegsman[3], P. Mason[4]

SUMMARY

Magmatic evolution of the Marowijne Greenstone Belt occurred in several phases during the Trans-Amazonian Orogeny. The first episode initiated the emplacement of the TTG-suites in multiple phases between 2.19 – 2.16 Ga and 2.15 – 2.11 Ga, during convergence and collision of the Amazonian and African cratons. TTG plutons that arose include the Brinck pluton, the Kabel Tonalite and the Saramacca batholith. Convergence during the second phase of the TTG magmatism, led to crustal processes resulting in the formation of the Tibiti biotite-granite from melts emerging from lithospheric structural acirvities, unrelated to subduction. Between 2.10 – 2.07 Ga another magmatic event presented itself, marking continuing convergence and the emplacement of syn-tectonic peraluminous granites such as the Phedra and the Patamacca, and at a later - to post-collision stage, the formation of the Akinto Soela granite.

GEOLOGY

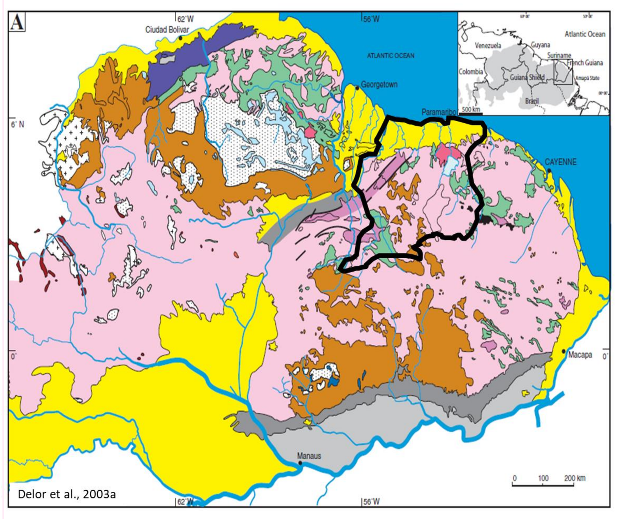

Figure 1: Simplified geological sketch map of the Guiana Shield (Delor et al., 2003a) with Suriname highlighted in black.

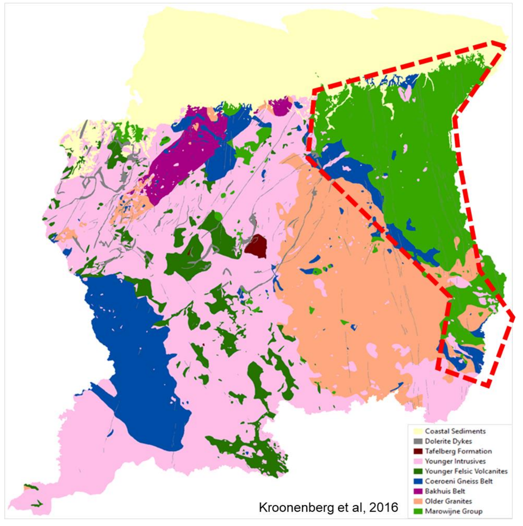

Figure 2: Simplified geological map of Suriname with the main units, after Bosma et al. (1977), modified by Kroonenberg et al. (2016).

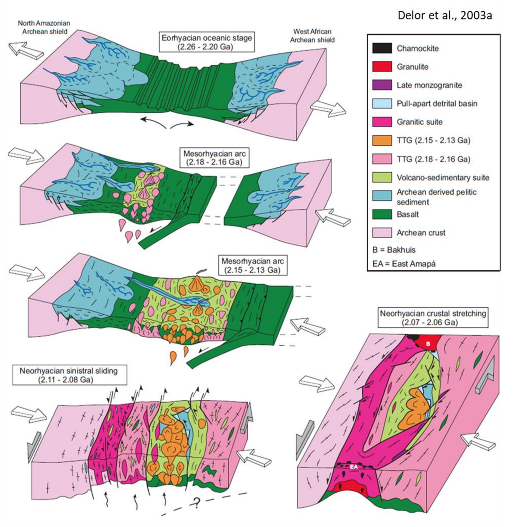

Figure 3: A geodynamic evolution model for the Guiana Shield (Delor et al., 2003a).

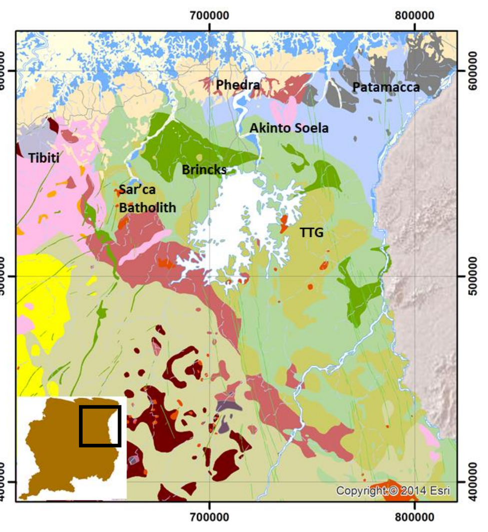

Figure 4: Geological map of the Suriname after Bosma et al. (1977) and Kroonenberg et al. (2016), with the locations of the granitoid of the Marowijne Greenstone Belt.

GEOCHEMICAL CLASSIFICATION

Magma Sources

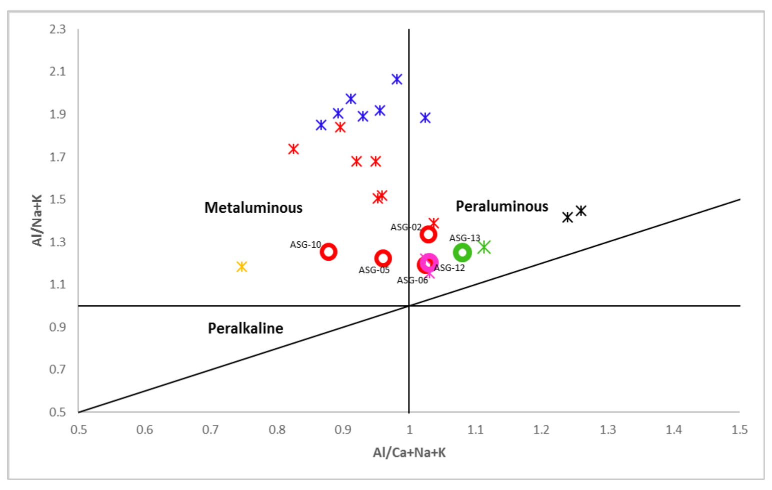

Figure 5: ASI-classification of the granitoid rocks after Shand (1947), with discrimination fields for different geochemical types of granitoids, after Maniar and Picolli (1989). The Akinto Soela granite plots in both the peraluminous and metaluminous fields. The Tibiti and Phedra granites both plot in the peraluminous fields.

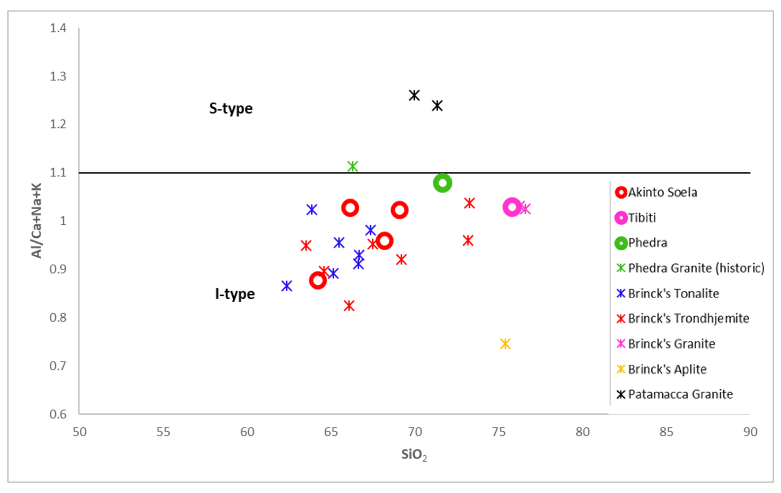

Figure 6: ASI-diagram (Al/Ca+Na+K vs SiO2) for the classification of the granitoids into I- and S-types, after Chappell and White (1974). The granitic samples studied in this report all plot as I-type with ASI values < 1.1.

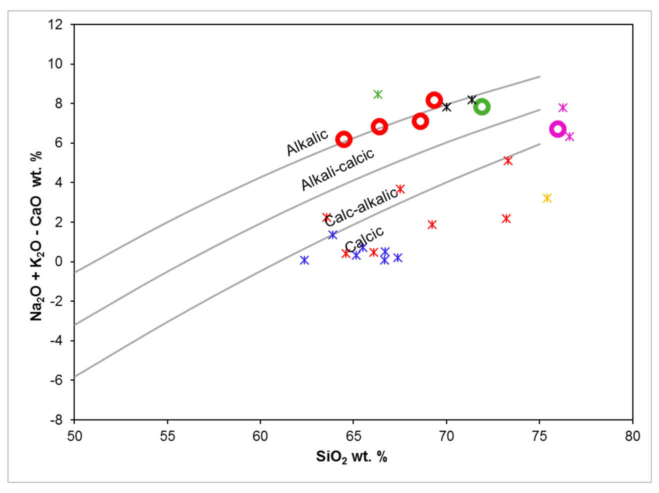

Figure 7: MALI index after Frost et al. (2001) illustrating the Akinto Soela and Phedra granites having an alkalic to alkali-calcic character, suggesting derivation from a sedimentary source, while the Tibiti granite has a calc-alkalic character similar to the Brink pluton, suggesting derivation from mafic to intermediate sources.

Tectonic Setting

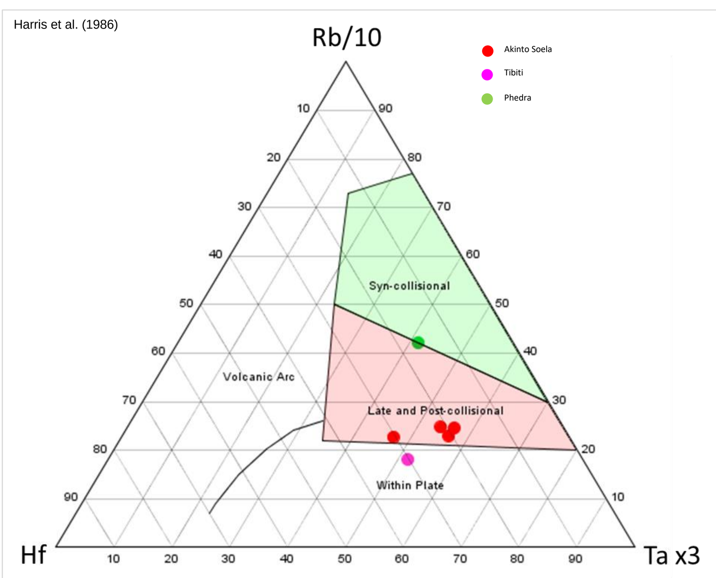

Figure 8: Rb-Hf-Ta triangular plot for acid-intermediate intrusive magmatism by Harris et al. (1986). The Akinto Soela granite (red) plotting as late and post collisional, the Tibiti granite as within plate and the Phedra granite on the border of the two collisional fields, but considered as syn-collisional,

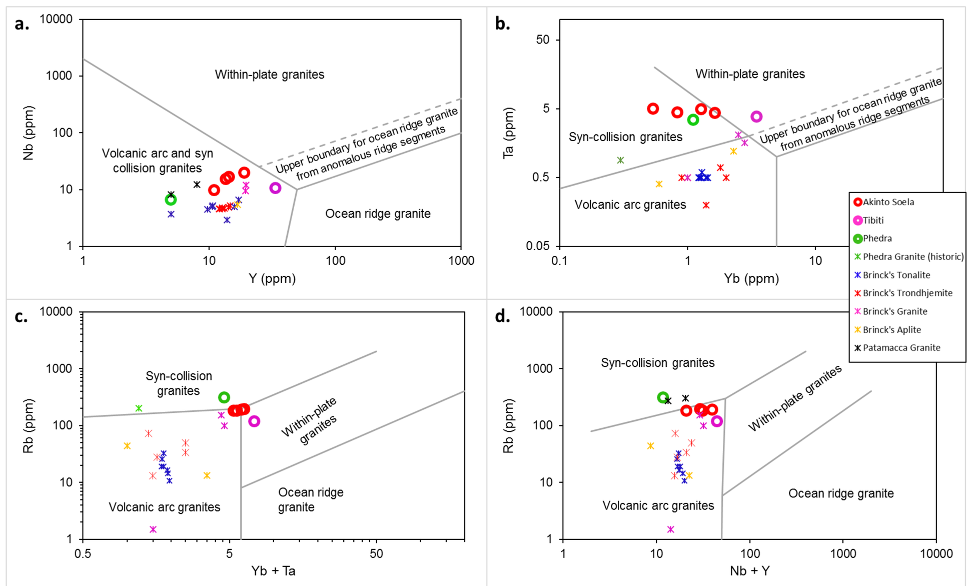

Figure 9: Tectonic discriminant diagrams after Pearce et al. (1984). a.) Nb-Y diagram in which all samples plot in the VAG and syn-COLG field. b.) Ta-Yb diagram showing the Akinto Soela and Phedra samples plotting as syn-COLG, and the Tibiti sample plotting as WPG. c.) Rb-(Yb+Ta) diagram illustrating the Tibiti sample plotting as a WPG, the Phedra sample as syn-COLG and the Akinto Soela samples occupying the triple corner of the WPG, the VAG and the syn-COLG fields. d.) Rb-(Nb+Y) diagram showing the Akinto Soela and Tibiti samples plotting as VAG and the Phedra sample plotting as syn-COLG.

REE and Spider Diagram

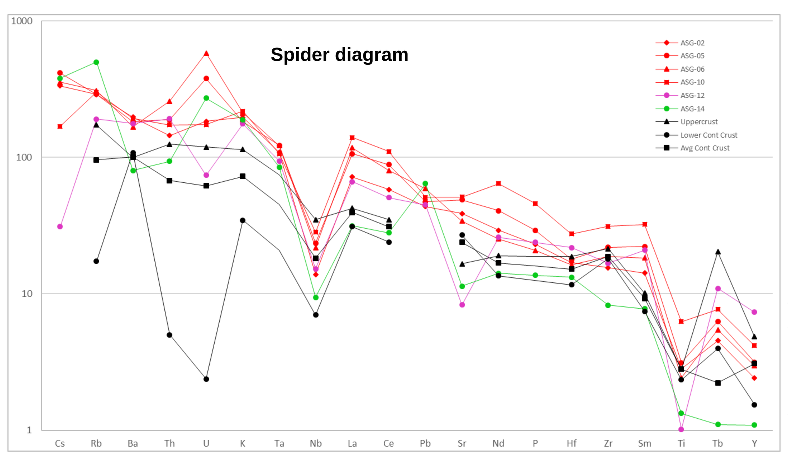

Figure 10: Spider diagram after Sun and McDonough (1992) normalized to a primordial mantle. The granitic samples mostly reflect influences from the uppercrust with minor element concentrations similar to the average continental crust.

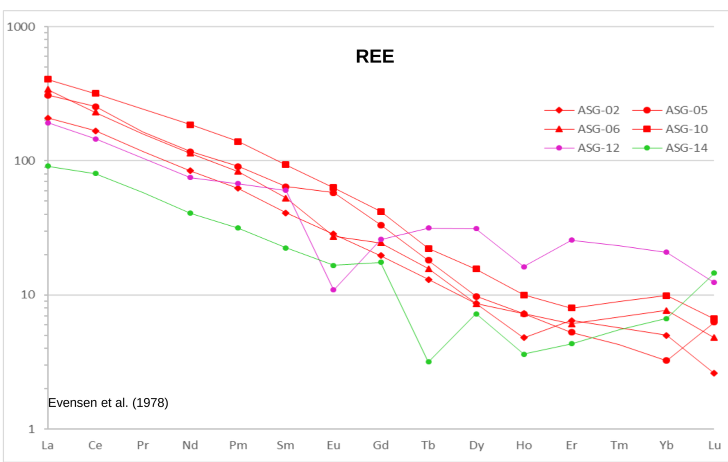

Figure 11: REE patterns of the Akinto Soela (red), Phedra (green) and Tibiti (magenta) granites, normalized to an average CI chondrite, after Evensen et al. (1978).

TIBITI GRANITE

This Tibiti granite is classified as a peraluminous, calc-alkalic, I-type biotite-granite, derived from mafic to intermediate sources by possible fractional crystallization. The age of unit (~2119 Ma), suggests emplacement during the second phase of TTG plutonism, within a continental plate setting, as the result of lithospheric structural activity, unrelated to subduction.

This unit is not considered part of the TTG-group as trace element concentrations show compositional variation.

Figure 12: Photographs of the pink Tibiti granite. The left photograph shows a weak banded texture in the rock and the right photograph, the medium to coarse grained texture is presented.

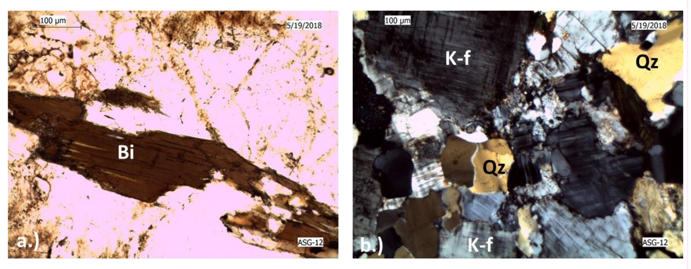

Figure 13: Microphotographs of thin sections from the Tibiti granite. a.) Reddish-brown biotite grain showing weak pleochroïc halos. b.) Rock forming minerals of the Tibiti Granite, including quartz and k-feldspars.

PHEDRA GRANITE

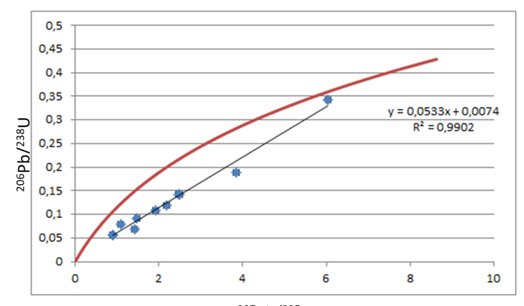

Figure 14: Concordia diagram of the Phedra zircon measurements. Data processed by Dr. Kriegsman (report in progress).

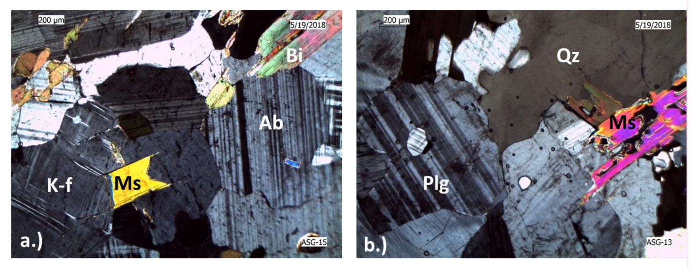

Figure 15: Microphotographs of thin sections from the Phedra granite. a.) Coarse grains of K-felspar with biotite and muscovite plates. b.) Large grains of the rock forming minerals quartz, plagioclase, muscovite and biotite.

The Phedra granite is classified as a peraluminous, alkali-calcic S-type two- mica granite, derived from melting sedimentary sources and emplaced within a syn-collisional tectonic environment. This unit has the most in common with the Patamacca granite.

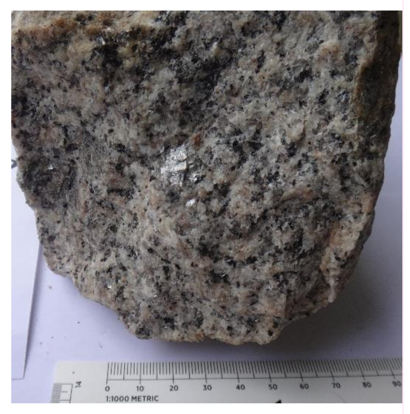

Figure 16: Sample of the Phedra granite collected along an abandoned quarry.

AKINTO SOELA GRANITE

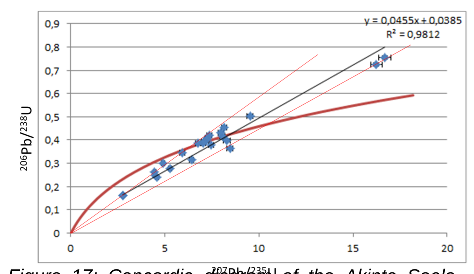

Figure 17: Concordia diagram of the Akinto Soela zircon measurements. Data processed by Dr. Kriegsman (report in progress).

Figure 18: Left photograph shows a boulder of the granite with geologist for scale and the photograph on the right shows drill core samples of the Akinto Soela granite, clearly showing the well-defined K-megacrysts in a coarse-grained texture

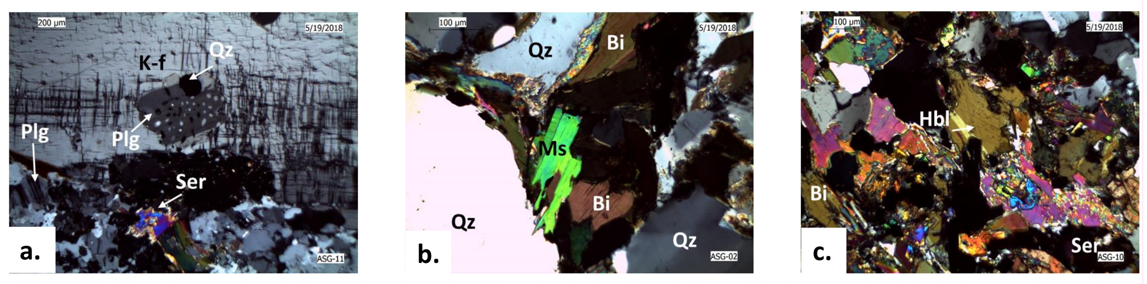

Figure 19: Microphotographs of thin sections from the Akinto Soela Granite. a.) Myrmekitic intergrowth of plagioclase and quartz in a K-feldspar megacryst. b.) Muscovite and biotite minerals. c.) Hornblende mineral.

The Akinto Soela granite is classified as an alkalic to alkali-calcic granite derived sedimentary sources with contamination of mafic rock material, hence the per- and metaluminous nature. This unit is the youngest magmatic occurrence yet, in the MGB, emplaced during late- to post collision events.

REFERENCES

Bosma, W., Kroonenberg, S. B., Van Lissa, R. V., Maas, K., & De Roever, E. W. F. (1977). Geological Map of Suriname. Geological and Mining Service of Suriname.

Chappell, B. W., & White, A. J. R. (1998). High- and Low-Temperature I-type Granites. Resource geology, volume 48, no. 4: pp 225 – 235.

Delor, C., Egal, E., Lafon, J. M., Cocherie, A., Guerrot, C., Rossi, P., Truffert, C., Theveniaut, H., Phillips, D. & Avelar V. G. (2003). Transamazonian crustal growth and reworking as revealed by the 1:500,000-scale geological map of French Guiana (2nd edition), Géologie De La France No 2-3-4: pp. 5 – 57.

Evensen, N.M., Hamilton, P. J. & O' Nions, R. K. (1978). Rare-earth abundances in chondritic meteorites. Geochim. Cosmochim. Acta, 42: pp. 1199 – 1211.

Frost, R., Barnes, C., Collins, W., Arculus, R., Ellis, D. & Frost, C. (2001). A Geochemical Classification for Granitic Rocks. Journal of Petrology, Volume 42: pp 2033 – 2048.

Harris. N. B. W., Pearce. J. A. & Tindle, A. G. (1986). Geochemical characteristics of collision-zone magmatism. Geological Society, London, Special Publications 19 (1): pp. 67 – 81.

Kroonenberg, S. B., de Roever, E. W. F., Fraga, L. M., Reis, N. J., Faraco, T., Lafon, J.-M. & Wong, T. E. (2016). Paleoproterozoic evolution of the Guiana Shield in Suriname: A revised model. Netherlands Journal of Geosciences: pp. 1 – 32.

Maniar, P. D. & Piccoli, P. M. (1989). Tectonic discrimination of granitoids. Geological Society of America Bulletin, 101: pp. 635 – 643.

Pearce, J.A., Harris N. B. W. & Tindle A. G. (1984). Trace element Discrimination Diagrams for the Tectonic Interpretation of Granitic Rocks: Journal of Petrology, 25: pp. 956 – 983.

Shand, S.J. (1947). Eruptive Rocks. Eruptive rocks, their genesis, composition, classification, and their relation to ore deposits, with a chapter on meteorites. (3rd ed): pp. 488.

Sun, S. S. & McDonough, W. F. (1989). Chemical and isotopic systematics of oceanic basalts: implications for mantle composition and processes. Geological Society, London, Special Publications, 42: pp. 313 – 345.

RECOMMENDATION

Additional analyses of the granitoids, especially the Tibiti and Phedra units, for more reliable interpretations

Reprocessing of zircon age dating results with the correction of “common” non-radiogenic Pb (204Pb) to eliminate uncertainties

Evaluation of other isolated granitoid occurrences in the Marowijne Greenstone Belt to find possible deposits of Sn, Li, Be and REEs

Isotopic studies, of both radiogenic and oxygen isotopes, on granitoids and nearby gold occurrences to understand fluid pathways and sources

THE MAGMATIC EVOLUTION OF THE MAROWIJNE GREENSTONE BELT

a. Pre- to early collision magmatism of the TTG suites in multiple phases (2.19 – 2.11 Ga), as the result of oceanic lithospher subduction, including the Brinck pluton, Saramacca batholith, Kabel tonalite, etc.

b. Second phase of the TTG magmatism (2.15 – 2.11 Ga) and emplacement of within-plate granites (Tibiti granite) as the result of possible lithospheric structural activities, unrelated to subduction

c. Syn-collision magmatism resulting from crustal thickening and the emplacement of the peraluminous two-mica granites (2.10 – 2.08 Ga), such as the Patamacca and Phedra granites

d. Late- to post collision magmatism (Akinto Soela granite) resulting from possible crustal relaxation and subsidiary subduction (2.08 – 2.06 Ga)

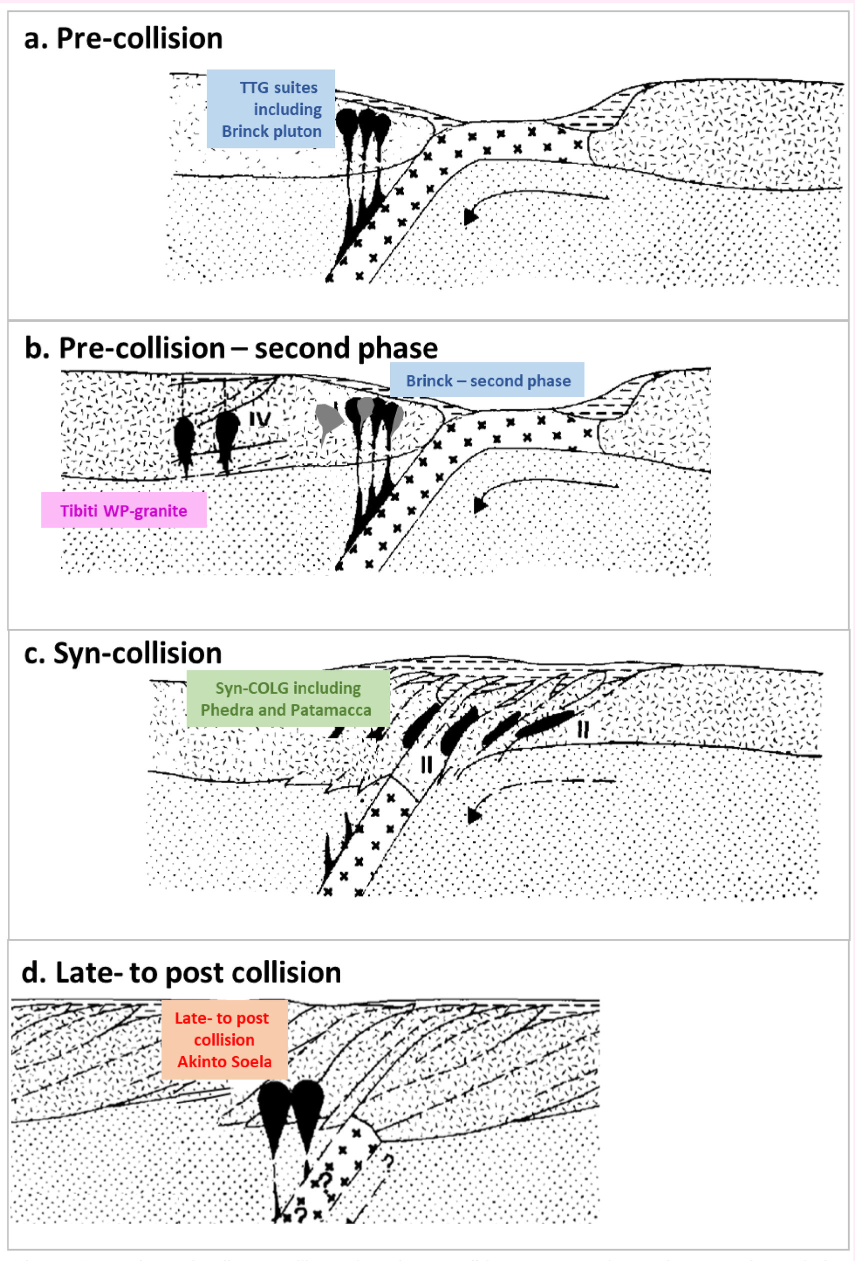

Figure 20: Schematic diagram illustrating the possible source regions of magmatism of the northeastern Marowijne Greenstone Belt, modified after Harris et al. (1998).

1. Anton de Kom University of Suriname, sam.kromopawiro@gmail.com; 2. Anton de Kom University of Suriname, salomonkroonenberg@gmail.com; 3. Naturalis Biodiversity Center, Leiden, the Netherlands, leo.kriegsman@naturalis.nl; 4. Institute of Earth Sciences, Utrecht University, the Netherlands, p.mason@uu.nl